


Article

Approximate Solution of PHI-Four and Allen–Cahn Equations Using Non-Polynomial Spline Technique

Mehboob Ul Haq ^{1,*}, Sirajul Haq ¹, Ihteram Ali ² and Mohammad Javad Ebadi ^{3,4,5,*} ¹ Faculty of Engineering Sciences, GIK Institute, Topi 23640, KP, Pakistan; siraj@giki.edu.pk² Department of Mathematics and Statistics, Women University Swabi, Swabi 23430, KP, Pakistan; ihteramali@wus.edu.pk³ Section of Mathematics, International Telematic University Uninettuno, Corso Vittorio Emanuele II, 39, 00186 Roma, Italy⁴ Department of Mathematics, Chababar Maritime University, Chababar 9971756499, Iran⁵ Department of Law, Economics and Human Sciences, Mediterranean University of Reggio Calabria, 89125 Reggio Calabria, Italy

* Correspondence: mehboob.haq@giki.edu.pk (M.U.H.); ebadi@cmu.ac.ir (M.J.E.)

Abstract: The aim of this work is to use an efficient and accurate numerical technique based on non-polynomial spline for the solution of the PHI-Four and Allen–Cahn equations. A recent discovery suggests that the PHI-Four equation focuses on its implications for particle physics and the behavior of scalar fields in the quantum realm. In materials science, ongoing research involves using the Allen–Cahn equation to understand and predict the evolution of microstructures in various materials as well as in biophysics. It depicts pattern formation in biological systems and the dynamics of spatial organization in tissues. To obtain an approximate solution of both equations, this technique uses forward differences for the time and cubic non-polynomial spline function for spatial discretization. The stability of the suggested technique is addressed using the von Neumann technique. Convergence test is carried out theoretically to show the order of convergence of the scheme. Some numerical tests are carried out to confirm accuracy and efficiency in terms of absolute error L_R . Convergence rates for different test problems are also computed numerically. Numerical results and simulations obtained are compared with the existing methods.



Citation: Haq, M.U.; Haq, S.; Ali, I.; Ebadi, M.J. Approximate Solution of PHI-Four and Allen–Cahn Equations using Non-Polynomial Spline Technique. *Mathematics* **2024**, *12*, 798. <https://doi.org/10.3390/math12060798>

Academic Editor: Rodica Luca

Received: 31 January 2024

Revised: 5 March 2024

Accepted: 6 March 2024

Published: 8 March 2024



Copyright: © 2024 by the authors. Licensee MDPI, Basel, Switzerland. This article is an open access article distributed under the terms and conditions of the Creative Commons Attribution (CC BY) license (<https://creativecommons.org/licenses/by/4.0/>).

Keywords: non-polynomial splines; Allen–Cahn equation; PHI-four equation; finite differences; von Neumann stability

MSC: 65D07

1. Introduction

Partial differential equations (PDEs) serve as a valuable tool for modeling a wide range of phenomena encountered in science and engineering. Their significance is evident in diverse fields including fluid dynamics, quantum theory and plasma physics [1].

We consider the following PDE [2]:

$$pu_t(x, t) + qu_{tt}(x, t) + ru_{xx}(x, t) + su(x, t) = f(u(x, t)), \quad a < x < b \quad \text{and} \quad t > 0, \quad (1)$$

with boundary and initial conditions

$$u(x, 0) = g_1(x), \quad u_t(x, 0) = qg_2(x), \quad a \leq x \leq b \quad (2)$$

$$u(a, t) = l_1(t), \quad u(b, t) = l_2(t). \quad (3)$$

In the above equation, u denotes wave displacement at particular position x with time t . Constants p, q, r, s are known parameters. The force term $f(u(x, t))$ characterizes external influences on the system.

Numerous types of equations may be constructed by altering the values of involved constants and force term in Equation (1). As an example, if we set $p = 0, q = 1, r = -1, s = -1$ and $f(u(x, t)) = -u^3$, then (1) becomes a PHI-Four equation. This equation holds significant importance in the field of mathematical physics and Cosmology. Triki and Wazwaz investigated the exact solution for bright and dark solitons and they also used the technique “sine–cosine ansatz” to find the solutions of more than one type of PHI-Four equations [1]. The authors in [3] explored a novel set of solutions for a generalized Fitzhugh Nagumo model using ansatz and tanh methods.

Furthermore, by taking the values of parameters $p = 1, q = 0, r = -1, s = -1$ and $f(u(x, t)) = -u^3$, Equation (1) transforms to an Allen–Cahn equation. The Allen–Cahn equation serves as a versatile model with applications across diverse fields, including bi-mathematics, plasma-physics, quantum mechanics and image processing [4–6]. The authors in [7] studied the Jacobi Gauss Lobatto technique to solve the PHI-Four model. Ehsani et al. [8] applied the homotopy perturbation method to solve a PHI-Four equation. The authors employed the solitary wave ansatz method to derive soliton solutions for a PHI-Four model with non-topological and topological nature in [9]. Alofi introduced a generalized tanh method to obtain solutions of both the Drinfeld–Sokolov system and the PHI-Four model in [10]. The authors in [11] formulated the latest solutions for Boussinesq, RLW and PHI-Four models. Sassaman and Biswas employed the soliton perturbation theory to explore solutions for both the Klein–Gordon and PHI-Four equations. Najafi investigated the soliton solution of the aforementioned equation utilizing He’s variational method [12].

The PHI-Four model is used in Cosmology, helping in understanding the evolution of the universe and the formation of cosmic structures. This model has also been used in statistical physics to study critical phenomena such as the behavior of a system near its critical point. The authors in [4–6] studied a wavelet-based method for solving Newell–Whitehead and Allen–Cahn equations. Considering non-periodic boundary conditions, the Allen–Cahn equation was solved by Ishtiaq et al. [13]. In condensed matter physics, the Allen–Cahn equation finds application in depicting phase transitions within materials. It has been applied in image processing for denoising and image segmentation in computer science. The Allen–Cahn equation has also been applied to model pattern formation in biological systems, such as formation of spatial patterns in the animal coat. Both equations are applied to study the dynamics of defects in materials.

The inception of spline approximation, in its current manifestation, can be traced back to the pioneering work of Schoenberg in 1946 [14]. Up to 1960, there was some research that mentioned spline functions. A few of the major figures in the development of spline are Ahlberg and Nilson [15], Birkhoff and Garabedian [16], Loscalzo and Talbot [17], Malaren [18], Rubin and Khosla [19] and Schoenberg [20]. Sokolnikoff (1956) offered a succinct but highly readable history of the evolution of beam theory. Some of the pioneers in the utilization of spline functions for achieving smooth numerical solutions to ordinary differential equations (ODEs) and partial differential equations (PDEs) are presented in [21–28]. The non-polynomial spline approach has been used more often recently to solve partial and ordinary differential equations. The work in [29–34] explains the numerical solutions of a system of second-order differential equations using non-polynomial splines, fourth-order problems using B splines and singular boundary value problems. Research on the fifth order can be found in Islam et al. [35], Siddiqi and Akram [36] and Siddiqi et al. [37]. The work of Akram and Siddiqi [38] yields sixth-order BVPs. According to Ramadan et al. [39], Rashidinia and Mahmoodi [40], non-polynomial splines can be used to solve parabolic equations numerically. For the solution of fifth-order boundary value problems, Kasi and Ballem [41] employed the finite element approach incorporating the Galerkin method with the quartic B spline as the basis function. Alam et al. [42] studied the RBF approximation method for the time-fractional FitzHugh–Nagumo equation. Radmanesh and Ebadi [43]

used the local RBF method for solving fractional integral equations. The authors in [44] solved the fractional fascioliasis disease model by Fibonacci polynomials.

The spline method stands out due to its numerous advantages in comparison to other numerical approaches. It provides a complete description of both function and its rate of change throughout the entire interval. In contrast, the finite difference method only provides functional values at specified knots, while the finite element method necessitates the computation of quadrature, which is not a requirement in the spline method. However, undesirable oscillations of these functions may be expected between the data points. It is important to note that splines of lower orders may result in reduced accuracy, while higher-order splines can lead to an increase in computational cost. The addition of tension to the polynomial splines overcomes this problem. Non-polynomial or tension splines were first introduced by Daniel G. Schweikert [45]. These splines were designed to get rid of extraneous inflection points in curve fitting [46]. The desirable scheme could be derived by choosing various tension parameter values over the domain. Finally, by applying non-polynomial splines, we can increase accuracy while using the same computing effort [47]. The paper’s outline is as follows. In Section 2, derivation and discretization of the proposed method is provided. In Section 3, stability of the method is explained using the von Neumann technique, and convergence analysis is discussed in detail. Accuracy and efficiency of the suggested methodology is shown by studying several mathematical problems in Section 4. Lastly, Section 5 includes the concluding remarks of the study.

2. The Proposed Methodology

In this portion, the proposed method is discussed, utilized to study the approximate solution of the hyperbolic telegraph equation. For this purpose, first, we transform (1) into the system of equations given below:

$$v(x, t) = u_t(x, t), \tag{4}$$

$$qv_t(x, t) + pv(x, t) + su = -ru_{xx} + f(u(x, t)), \tag{5}$$

with conditions

$$u(x, 0) = g_1(x), \quad u_t(x, 0) = qg_2(x), \tag{6}$$

$$u(a, t) = l_1(t), \quad u(b, t) = l_2(t). \tag{7}$$

Using finite difference for the temporal part and a θ -weighted scheme for the spatial part of Systems (4) and (5), the following equations can be derived:

$$\frac{u^{n+1} - u^n}{k} = \theta v^{n+1} + (1 - \theta)v^n, \tag{8}$$

$$q \frac{v^{n+1} - v^n}{k} + \theta [pv^{n+1} + su^{n+1} + ru_{xx}^{n+1}] + (1 - \theta)[pv^n + su^n + ru_{xx}^n] - f(u(x, t^n)) = 0, \tag{9}$$

where $v^n = v(x, t^n)$, $u^n = u(x, t^n)$, $t^{n+1} = t^n + k$ and k is the time step. Substituting $\theta = \frac{1}{2}$, we can obtain

$$q \frac{v^{n+1} - v^n}{k} + p \frac{v^{n+1} + v^n}{2} + s \frac{u^{n+1} + u^n}{2} + r \frac{u_{xx}^{n+1} + u_{xx}^n}{2} - f(u(x, t^n)) = 0.$$

Equivalently, the above equation can be written as

$$u_{xx}^{n+1} + u_{xx}^n = \frac{2q}{rk}(v^{n+1} - v^n) - \frac{p}{r}(v^{n+1} + v^n) - \frac{s}{r}(u^{n+1} + u^n) + \frac{2}{rk}f(u(x, t^n)). \tag{10}$$

In order to find the approximate solution of the system under consideration, the technique of non-polynomial splines is implemented.

For this goal, first, we define a partition in $[a, b]$ given by $\Omega : a = x_0 < x_1 < x_2 < \dots < x_{N-1} < x_N = b$, where $x_j = a + jh$, $j = 0, 1, 2, \dots, N$ and h is the step size.

For the solution of Equation (1), the unknown $u(x, t^n)$ is approximated by $U^n(x)$ using the non-polynomial splines as follows:

$$U^n(x) = P^n(x), \quad x_j \leq x \leq x_{j+1}, \quad j = 0, 1, 2, \dots, N - 1. \tag{11}$$

In the above equation,

$$P^n(x) = P_j(x, t_n) = d_j(t_n) + (x - x_j)c_j(t_n) + \sin \omega(x - x_j)a_j(t_n) + \cos \omega(x - x_j)b_j(t_n), \tag{12}$$

where a_j, b_j, c_j, d_j are unknowns to be determined. According to the definition of splines,

$$U_j^n = P_j(x_j, t_n), \quad U_{j+1}^n = P_{j+1}(x_{j+1}, t_n). \tag{13}$$

From Equations (12) and (13), the following relations can be obtained:

$$\begin{aligned} b_j + d_j &= U_j^n, & a_j \sin \omega h + b_j \cos \omega h + c_j h + d_j &= U_{j+1}^n, & -b_j \omega^2 &= S_j^n, \\ & & & & -a_j \omega^2 \sin \theta - b_j \omega^2 \cos \theta &= S_{j+1}^n, \end{aligned} \tag{14}$$

where $S_j^n = U_{xx}(x_j)$. Now, from Equation (14), we can obtain

$$\begin{aligned} b_j &= -\frac{1}{\omega^2} S_j^n, & d_j &= \frac{1}{\omega^2} S_j^n + U_j^n, & c_j &= \frac{U_{j+1}^n - U_j^n}{h} + \frac{S_{j+1}^n - S_j^n}{\omega^2 h^2}, \\ & & & & a_j &= \frac{\cos \omega h}{\omega^2 \sin \omega h} S_j^n - \frac{1}{\omega^2 \sin \omega h} S_{j+1}^n. \end{aligned} \tag{15}$$

The use of condition $P'_{j-1}(x_j, t^n) = P'_j(x_j, t^n)$ produces

$$\omega a_j + c_j = \omega a_{j-1} \cos \omega h - \omega b_{j-1} \sin \omega h + c_{j-1}, \quad j = 1, 2, \dots, N - 1. \tag{16}$$

Putting values from Equation (15) in Equation (16), the following recurrence relation can be obtained:

$$U_{j+1}^n - 2U_j^n + U_{j-1}^n = \alpha_1 S_{j+1}^n + 2\beta_1 S_j^n + \alpha_1 S_{j-1}^n; \quad j = 1, 2, \dots, N - 1, \tag{17}$$

where

$$\alpha_1 = \frac{h}{\omega \sin \omega h} - \frac{1}{\omega^2}, \quad \beta_1 = \frac{2}{\omega^2} - \frac{2h \cos \omega h}{\omega \sin \omega h}.$$

Combining Equation (17) at time levels n and $n + 1$, a newly obtained equation is given by

$$\begin{aligned} (U_{j+1}^{n+1} + U_{j+1}^n) - 2(U_j^{n+1} + U_j^n) + (U_{j-1}^{n+1} + U_{j-1}^n) &= \alpha_1(S_{j+1}^{n+1} + S_{j+1}^n) + 2\beta_1(S_j^{n+1} + S_j^n) \\ &+ \alpha_1(S_{j-1}^{n+1} + S_{j-1}^n); \quad j = 1, 2, \dots, N - 1. \end{aligned} \tag{18}$$

Now, substituting values from (10) in (18), we can obtain

$$\begin{aligned} A_1 U_{j+1}^{n+1} + A_2 U_j^{n+1} + A_3 U_{j-1}^{n+1} + A_4 V_{j+1}^{n+1} + A_5 V_j^{n+1} + A_6 V_{j-1}^{n+1} \\ = B_1 U_{j+1}^n + B_2 U_j^n + B_3 U_{j-1}^n + B_4 V_{j+1}^n + B_5 V_j^n + B_6 V_{j-1}^n. \end{aligned} \tag{19}$$

The coefficients involved in (19) are given as follows:

$$\begin{aligned} A_1 &= 1 + \frac{\alpha_1 s}{r}, & A_2 &= -2 + \frac{2\beta_1 s}{r}, & A_3 &= 1 + \frac{\alpha_1 s}{r}, \\ A_4 &= -\frac{2\alpha_1 q}{rk} + \frac{\alpha_1 p}{r}, & A_5 &= -\frac{4\beta_1 q}{rk} - \frac{2\beta_1 p}{r}, & A_6 &= -\frac{2\alpha_1 q}{rk} + \frac{\alpha_1 p}{r}. \end{aligned}$$

$$B_1 = -1 - \frac{\alpha_1 s}{r}, \quad B_2 = 2 - \frac{2\beta_1 s}{r}, \quad B_3 = -1 - \frac{\alpha_1 s}{r},$$

$$B_4 = -\frac{2\alpha_1 q}{rk} - \frac{\alpha_1 p}{r}, \quad B_5 = -\frac{4\beta_1 q}{rk} - \frac{2\beta_1 p}{r}, \quad B_6 = -\frac{2\alpha_1 q}{rk} - \frac{\alpha_1 p}{r}.$$

For finding the solution of the system, Equations (8) and (19) along with conditions given in Equations (6) and (7) are used.

3. Stability of the Method

In this section, the stability of the scheme is discussed using the von Neumann technique. For this purpose, let us assume

$$U_j^n = A\eta^n \exp(ij\phi), \quad V_j^n = B\eta^n \exp(ij\phi), \quad W = \frac{\eta^{n+1}}{\eta^n}, \tag{20}$$

where A and B are harmonic amplitudes, $\phi = kh$ is the wave number, k is the mode number and W is the amplification factor of the scheme. The use of Equation (20) in (19) gives rise to

$$\frac{\eta^{n+1}}{\eta^n} = \frac{B_1 A \exp(i\phi) + B_2 A + B_3 A \exp(-i\phi) + B_4 B \exp(i\phi) + B_5 B + B_6 B \exp(-i\phi)}{A_1 A \exp(i\phi) + A_2 A + A_3 A \exp(-i\phi) + A_4 B \exp(i\phi) + A_5 B + A_6 B \exp(-i\phi)}. \tag{21}$$

Substituting the values of $A_k, k = 1, 2, \dots, 6$ and $B_k, k = 1, 2, \dots, 6$ the above equation takes the form

$$\eta^{n+1} \left[-2A \cos(\phi) - \frac{2A\alpha_1 s}{r} \cos(\phi) + 2A - \frac{2A\beta_1 s}{r} - \frac{4B\alpha_1 q}{rk} \cos(\phi) - \frac{2B\alpha_1 p}{r} \cos(\phi) - \frac{4B\beta_1 q}{rk} - \frac{2B\beta_1 p}{r} \right]$$

$$= \eta^{n+1} \left[2A \cos(\phi) + \frac{2A\alpha_1 s}{r} \cos(\phi) - 2A + \frac{2A\beta_1 s}{r} - \frac{4B\alpha_1 q}{rk} \cos(\phi) + \frac{2B\alpha_1 p}{r} \cos(\phi) + \frac{4B\beta_1 q}{rk} - \frac{2B\beta_1 p}{r} \right],$$

$$\eta^{n+1} [z_1 + z_2] = \eta^n [-z_1 + z_2]. \tag{22}$$

where $z_1 = 2A \cos(\phi) + \frac{2A\alpha_1 s}{r} \cos(\phi) - 2A + \frac{2A\beta_1 s}{r} + \frac{2B\alpha_1 p}{r} \cos(\phi) + \frac{4B\beta_1 q}{rk}$, $z_2 = -\frac{4B\alpha_1 q}{rk} \cos(\phi) - \frac{2B\beta_1 p}{r}$.

Therefore,

$$W = \frac{w_1 + ix_1}{w_2 - ix_2}, \tag{23}$$

where

$$w_1 = -z_1 + z_2,$$

$$w_2 = z_1 + z_2,$$

$$x_1 = x_2 = 0.$$

From Equation (23), it can be observed that $|W| \leq 1$, and hence the scheme is unconditionally stable.

Convergence Test

The local truncation error for Scheme (17) is given by

$$T_j = y_{j+1} - 2y_j + y_{j-1} - h^2(\alpha_1 y''_{j+1} + 2\beta_1 y''_j + \alpha_1 y''_{j-1}). \tag{24}$$

Expanding the terms by Taylor’s series, we obtain

$$y_{j+1} = y_j + hy'_j + \frac{h^2}{2!}y''_j + \frac{h^3}{3!}y'''_j + \frac{h^4}{4!}y^{(4)}_j + \frac{h^5}{5!}y^{(5)}_j + \frac{h^6}{6!}y^{(6)}_j + \frac{h^7}{7!}y^{(7)}_j + \frac{h^8}{8!}y^{(8)}_j + \dots \quad (25)$$

$$y_{j-1} = y_j - hy'_j + \frac{h^2}{2!}y''_j - \frac{h^3}{3!}y'''_j + \frac{h^4}{4!}y^{(4)}_j - \frac{h^5}{5!}y^{(5)}_j + \frac{h^6}{6!}y^{(6)}_j - \frac{h^7}{7!}y^{(7)}_j + \frac{h^8}{8!}y^{(8)}_j - \dots \quad (26)$$

$$y''_{j+1} = y''_j + hy'''_j + \frac{h^2}{2!}y^{(4)}_j + \frac{h^3}{3!}y^{(5)}_j + \frac{h^4}{4!}y^{(6)}_j + \frac{h^5}{5!}y^{(7)}_j + \dots \quad (27)$$

$$y''_{j-1} = y''_j - hy'''_j + \frac{h^2}{2!}y^{(4)}_j - \frac{h^3}{3!}y^{(5)}_j + \frac{h^4}{4!}y^{(6)}_j - \frac{h^5}{5!}y^{(7)}_j + \dots \quad (28)$$

By substituting the values from Equations (25)–(28) in Equation (24) after simplification, we obtain

$$T_j = h^2y''_j + \frac{2h^4}{4!}y^{(4)}_j + \frac{2h^6}{6!}y^{(6)}_j - h^2 \left[\alpha_1 \left(y'_j + \frac{h^2}{2!}y^{(4)}_j + \frac{h^4}{4!}y^{(6)}_j \right) + 2\beta_1y''_j \right] \quad (29)$$

$$+ \alpha_1 \left(y'_j + \frac{h^2}{2!}y^{(4)}_j + \frac{h^4}{4!}y^{(6)}_j \right) \Big]. \quad (30)$$

After some algebraic manipulation, we have

$$T_j = \left(1 - 2\alpha_1 - 2\beta_1 \right) h^2y''_j + \left(\frac{1}{12} - \alpha_1 \right) h^4y^{(4)}_j + \left(\frac{1}{360} - \frac{\alpha_1}{12} \right) h^6y^{(6)}_j. \quad (31)$$

When $h = 0$, the truncation error vanishes. The lowest power of h that makes the error equal to zero is h^2 . Hence, this implies that the method is a second-order convergent $O(h^2)$. To obtain the fourth-order convergent scheme, we equate the coefficient equations to zero given below:

$$1 - 2\alpha_1 - 2\beta_1 = 0, \\ 1 - 12\alpha_1 = 0.$$

Upon solving for the values of α_1, β_1 , we obtain $\alpha_1 = \frac{1}{12}$ and $\beta_1 = \frac{5}{12}$, which allows us to deduce that the method is $O(h^4)$ -convergent. Similarly, we can derive the values of $\alpha_1 = \frac{1}{30}$ and $\beta_1 = \frac{7}{15}$, which shows the $O(h^6)$ convergence of the method.

4. Examples

In this section, three examples are studied to check efficiency and validity of the suggested scheme. The results are tested via absolute error L_R and L_∞ defined as follows:

$$L_R = |X_j^n - X^{*n}_j|, \\ L_\infty = \max |X_j^n - X^{*n}_j|. \quad (32)$$

where X^* and X are approximate and exact solutions, respectively, of the problem under consideration, and n stands for the n th time level.

4.1. Example 1

We consider a particular case of (1) where $p = 0, q = 1, r = -1, s = -1$ and $f(u(x, t)) = -u^3$ in $(0, 1)$ given by

$$u_{tt}(x, t) - u_{xx}(x, t) - u(x, t) = -u^3, \quad (33)$$

with initial conditions (ICs) and boundary conditions (BCs)

$$\begin{aligned}
 u(x, 0) &= 0 \quad \text{and} \quad u_t(x, 0) = x, \quad 0 < x < 1, \\
 u(0, t) &= 0, \\
 u(1, t) &= t + \frac{t^3}{6} - \frac{t^5}{20} + \frac{t^5}{120} - \frac{t^7}{140} - \frac{t^7}{840} - \frac{t^{11}}{23760} + \frac{t^{13}}{37440} - \frac{t^{15}}{168000} + \frac{t^{17}}{2176000}, \quad t \geq 0.
 \end{aligned}$$

The exact solution of Equation (33) is given in [8]

$$u(x, t) = xt + \frac{xt^3}{6} - \frac{x^3t^5}{20} + \frac{xt^5}{120} - \frac{xt^7}{140} - \frac{x^3t^7}{840} - \frac{x^3t^{11}}{23760} + \frac{x^5t^{13}}{37440} - \frac{x^7t^{15}}{168000} + \frac{x^9t^{17}}{2176000}.$$

In Table 1, we present absolute errors L_R with $h = 0.1$, $\Delta t = 0.002$. These error values are compared with those given in [2] for different spatial values and time levels. Figure 1 provides a visual comparison between two solutions for time $t = 0.01$ and $h = 0.1$, $\Delta t = 0.002$. In Figure 2, we plot a space–time graph up to $t = 0.01$ to depict how the solution profile evolves over time. From the table, it can be noticed that the results obtained using the proposed method are better and more accurate for $t = 0.002$ compared to the results of the method available in the literature. Figure 3 exhibits the error plot between exact and approximate solutions.

Table 1. L_R for Example 1, when $h = 0.1$, $\Delta t = 0.002$.

	x/t	0.002	0.004	0.006	0.008	0.01
[Present]	0	0.00	0.00	0.00	0.00	0.00
	0.1	1.43×10^{-16}	1.83×10^{-9}	8.42×10^{-9}	2.12×10^{-8}	4.32×10^{-8}
	0.2	2.86×10^{-16}	3.64×10^{-9}	1.67×10^{-8}	4.22×10^{-8}	8.58×10^{-8}
	0.3	4.36×10^{-16}	5.35×10^{-9}	2.46×10^{-8}	6.21×10^{-8}	1.26×10^{-7}
	0.4	5.41×10^{-16}	6.86×10^{-9}	3.16×10^{-8}	7.96×10^{-8}	1.62×10^{-7}
	0.5	5.81×10^{-16}	8.02×10^{-9}	3.69×10^{-8}	9.30×10^{-8}	1.89×10^{-7}
	0.6	6.12×10^{-16}	8.62×10^{-9}	3.97×10^{-8}	1.00×10^{-7}	2.04×10^{-7}
	0.7	5.48×10^{-16}	8.43×10^{-9}	3.88×10^{-8}	9.78×10^{-8}	1.99×10^{-7}
	0.8	5.52×10^{-16}	7.16×10^{-9}	3.29×10^{-8}	8.30×10^{-8}	1.69×10^{-7}
	0.9	2.61×10^{-16}	4.47×10^{-9}	2.06×10^{-8}	5.19×10^{-8}	1.06×10^{-7}
1	0.00	0.00	0.00	0.00	0.00	
[2]	0	0.00	0.00	0.00	0.00	0.00
	0.1	1.28×10^{-10}	6.75×10^{-10}	1.63×10^{-9}	2.98×10^{-9}	4.75×10^{-9}
	0.2	9.38×10^{-10}	2.70×10^{-9}	5.24×10^{-9}	8.55×10^{-9}	1.26×10^{-8}
	0.3	6.94×10^{-10}	1.08×10^{-10}	1.73×10^{-9}	4.83×10^{-9}	9.22×10^{-9}
	0.4	5.61×10^{-9}	1.28×10^{-8}	2.14×10^{-8}	3.15×10^{-8}	4.29×10^{-8}
	0.5	1.31×10^{-8}	2.39×10^{-8}	3.23×10^{-8}	3.82×10^{-8}	4.15×10^{-8}
	0.6	4.43×10^{-8}	9.06×10^{-8}	1.38×10^{-7}	1.87×10^{-7}	2.37×10^{-7}
	0.7	1.18×10^{-7}	2.32×10^{-7}	3.41×10^{-7}	4.45×10^{-7}	5.43×10^{-7}
	0.8	3.00×10^{-7}	6.01×10^{-7}	9.02×10^{-7}	1.20×10^{-6}	1.50×10^{-6}
	0.9	5.53×10^{-7}	1.10×10^{-6}	1.64×10^{-6}	2.17×10^{-6}	2.69×10^{-6}
1	0.00	0.00	0.00	0.00	0.00	

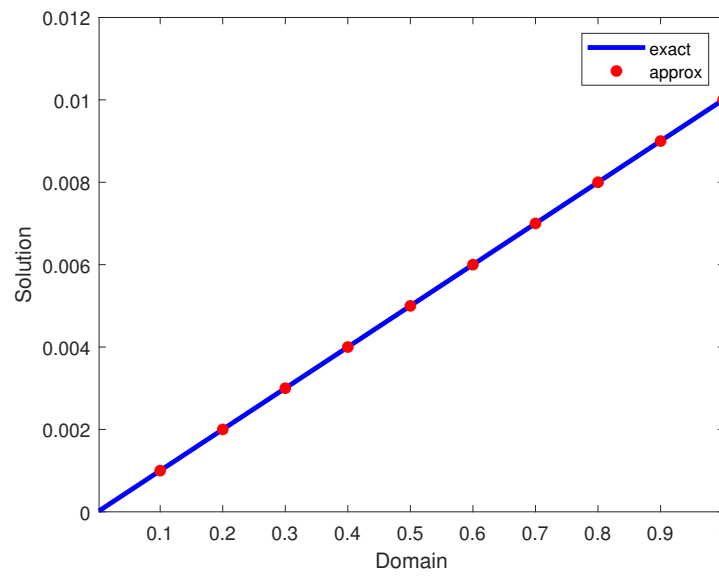


Figure 1. Approximate and exact solutions of Example 1 at various time levels when $\Delta t = 0.002$ and $h = 0.1$.

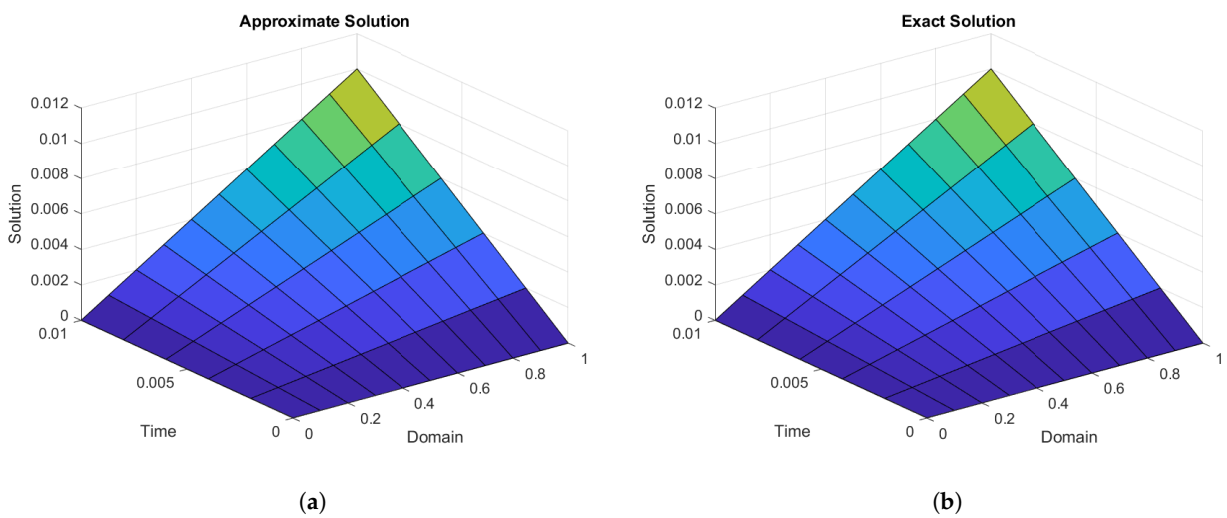


Figure 2. (a) Surface graph for approximate solution of Problem 1, when $t = 0.01$, $h = 0.1$. (b) Surface graph of the exact solution with $t = 0.01$ and $h = 0.1$.

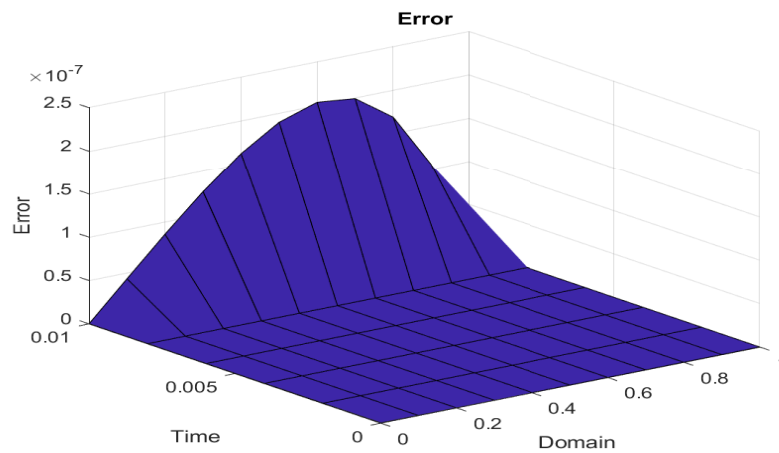


Figure 3. Absolute error of Example 1 when $\Delta t = 0.002$ and $h = 0.1$.

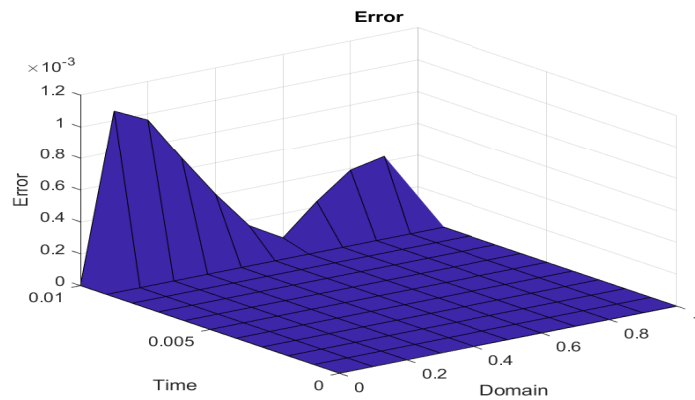


Figure 4. Absolute error of Problem 2 when $\Delta t = 0.001$ and $h = 0.1$.

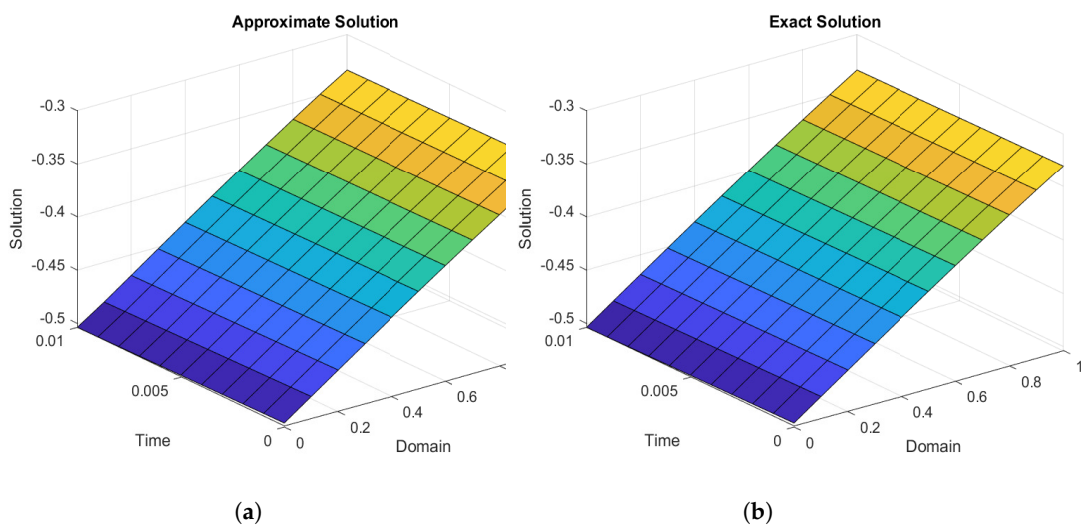


Figure 5. (a) Surface plot for numerical solution of Problem 2, when $h = 0.1, t = 0.01$. (b) Surface plot for the exact solution when $t = 0.01, h = 0.1$.

4.3. Example 3

In this example, we solve Equation (1), taking parameters $p = 1, q = 0, r = -1, s = -1$ and $f(u(x, t)) = -u^3$. The equation is defined within domain $0 < x < 1$ and $t > 0$ and is governed by the following ICs and BCs, respectively, given by

$$u_t(x, t) - u_{xx}(x, t) - u(x, t) = -u^3, \tag{39}$$

$$u(x, 0) = \left(1 + e^{-\left(\frac{\sqrt{2}}{2}\right)x}\right)^{-1}, \tag{40}$$

$$u(0, t) = \left(1 + e^{-\left(\frac{3}{2}\right)t}\right)^{-1}, \tag{41}$$

$$u(1, t) = \left(1 + e^{-\left(\frac{\sqrt{2}}{2}\right)\left(1 + \frac{3\sqrt{2}}{2}t\right)}\right)^{-1}. \tag{42}$$

The exact solution for the model equation is taken from [4]:

$$u(x, t) = \left(1 + e^{-\left(\frac{\sqrt{2}}{2}\right)\left(x + \frac{3\sqrt{2}}{2}t\right)}\right)^{-1}. \tag{43}$$

Table 3 presents the L_R for the selected values of $h = 0.1$ and $\Delta t = 0.001$. The obtained results are compared with the results of [2]. The table clearly indicates that the solutions obtained using the proposed method are in good accord with the existing methods in

the literature. Figure 6 displays the graphical representation of absolute error between both numerical and exact solutions at time $t = 0.01$. In Figure 7, we provide surface plots depicting the behavior of the numerical solution when $t = 0.01$.

Table 3. L_R for Example 3, when $h = 0.1, \Delta t = 0.001$.

	x/t	0.001	0.003	0.005	0.007	0.009	0.01
[Present]	0	3.75×10^{-4}	3.75×10^{-4}	3.75×10^{-4}	3.75×10^{-4}	3.75×10^{-4}	3.75×10^{-4}
	0.1	1.35×10^{-5}	6.31×10^{-5}	1.11×10^{-4}	1.43×10^{-4}	1.66×10^{-4}	1.75×10^{-4}
	0.2	4.01×10^{-7}	2.54×10^{-7}	1.30×10^{-5}	2.99×10^{-5}	4.68×10^{-5}	5.48×10^{-5}
	0.3	9.50×10^{-8}	4.91×10^{-7}	3.56×10^{-7}	2.37×10^{-6}	7.31×10^{-6}	1.04×10^{-5}
	0.4	7.57×10^{-8}	2.04×10^{-7}	4.42×10^{-7}	5.38×10^{-7}	4.76×10^{-8}	4.85×10^{-7}
	0.5	7.41×10^{-8}	2.24×10^{-7}	3.66×10^{-7}	5.30×10^{-7}	6.69×10^{-7}	6.94×10^{-7}
	0.6	7.12×10^{-8}	2.13×10^{-7}	3.55×10^{-7}	4.95×10^{-7}	6.39×10^{-7}	7.10×10^{-7}
	0.7	6.77×10^{-8}	2.03×10^{-7}	3.37×10^{-7}	4.70×10^{-7}	6.01×10^{-7}	6.66×10^{-7}
	0.8	6.35×10^{-8}	1.91×10^{-7}	3.14×10^{-7}	4.32×10^{-7}	5.44×10^{-7}	5.98×10^{-7}
	0.9	6.09×10^{-8}	1.65×10^{-7}	2.53×10^{-7}	3.30×10^{-7}	4.00×10^{-7}	4.33×10^{-7}
1	0.00	0.00	0.00	0.00	0.00	0.00	
[2]	0	0.00	0.00	0.00	0.00	0.00	0.00
	0.1	2.51×10^{-4}	7.07×10^{-4}	1.13×10^{-3}	1.53×10^{-3}	1.92×10^{-3}	2.11×10^{-3}
	0.2	3.35×10^{-4}	1.02×10^{-3}	1.72×10^{-3}	2.41×10^{-3}	3.10×10^{-3}	3.45×10^{-3}
	0.3	4.39×10^{-4}	1.33×10^{-3}	2.23×10^{-3}	3.15×10^{-3}	4.09×10^{-3}	4.56×10^{-3}
	0.4	5.46×10^{-4}	1.65×10^{-3}	2.77×10^{-3}	3.91×10^{-3}	5.06×10^{-3}	5.64×10^{-3}
	0.5	6.54×10^{-4}	1.98×10^{-3}	3.31×10^{-3}	4.67×10^{-3}	6.04×10^{-3}	6.74×10^{-3}
	0.6	7.63×10^{-4}	2.30×10^{-3}	3.86×10^{-3}	5.43×10^{-3}	7.03×10^{-3}	7.83×10^{-3}
	0.7	8.70×10^{-4}	2.62×10^{-3}	4.40×10^{-3}	6.19×10^{-3}	7.97×10^{-3}	8.85×10^{-3}
	0.8	9.65×10^{-4}	2.96×10^{-3}	4.90×10^{-3}	6.76×10^{-3}	8.51×10^{-3}	9.35×10^{-3}
	0.9	1.16×10^{-3}	3.06×10^{-3}	4.62×10^{-3}	5.95×10^{-3}	7.14×10^{-3}	7.69×10^{-3}
1	0.00	0.00	0.00	0.00	0.00	0.00	

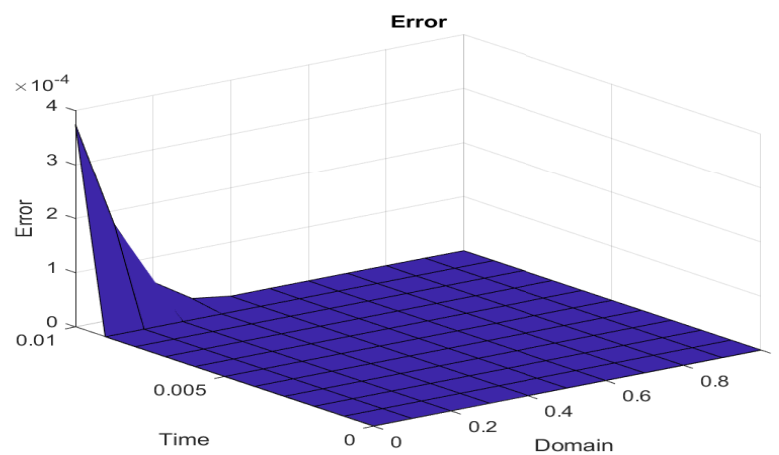


Figure 6. Absolute error of Problem 3 when $\Delta t = 0.001$ and $h = 0.1$.

The Tables 4 and 5 represent the convergence rate, i.e., $C.R = \frac{L_\infty(\Delta t_{i+1})}{L_\infty(\Delta t_i)}$ for the above Examples 2 and 3, respectively. In the aforementioned tables, we see the convergence rate with respect to time step size. Table 6 shows the values of L_R for Problem 3 when $t = 10, \Delta t = 0.1$ and step size $h = 0.1$. By examining the aforementioned table, we can see the performance of the method for higher time values. So we deduce that the method is working very well for much longer time, that is, $t \gg 0$. The surface plots for error and two solutions are simulated and shown in Figures 8 and 9, respectively.

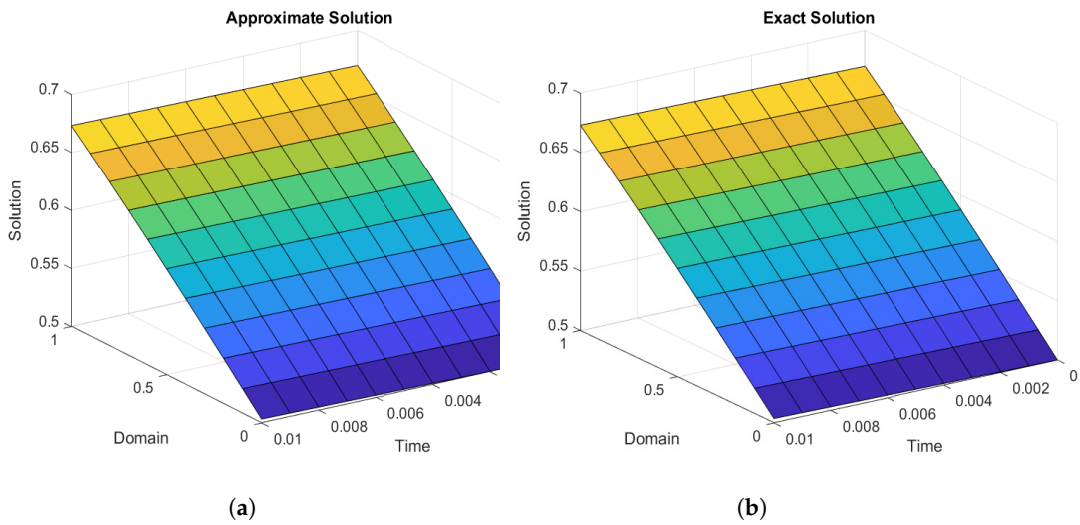


Figure 7. (a) Surface plot of approximate solution corresponding to Problem 3, when $t = 0.01$ and $h = 0.1$ (b) Surface plot of the exact solution with $t = 0.01, h = 0.1$.

Table 4. Convergence rates (CRs) for Example 2.

Δt	L_∞	C.R
1/100	1.06×10^{-3}	—
1/200	1.05×10^{-3}	9.91×10^{-1}
1/400	0.001054541	1.00
1/600	0.00105635	1.00
1/700	0.001056934	1.00
1/1000	0.001058059	1.00

Table 5. Convergence rates (CRs) for Example 3.

Δt	L_∞	C.R
1/100	3.75×10^{-3}	—
1/200	1.87×10^{-3}	5.00×10^{-1}
1/400	9.37×10^{-4}	5.00×10^{-1}
1/600	6.25×10^{-4}	6.67×10^{-1}
1/700	5.36×10^{-4}	8.57×10^{-1}
1/1000	3.75×10^{-4}	7.00×10^{-1}

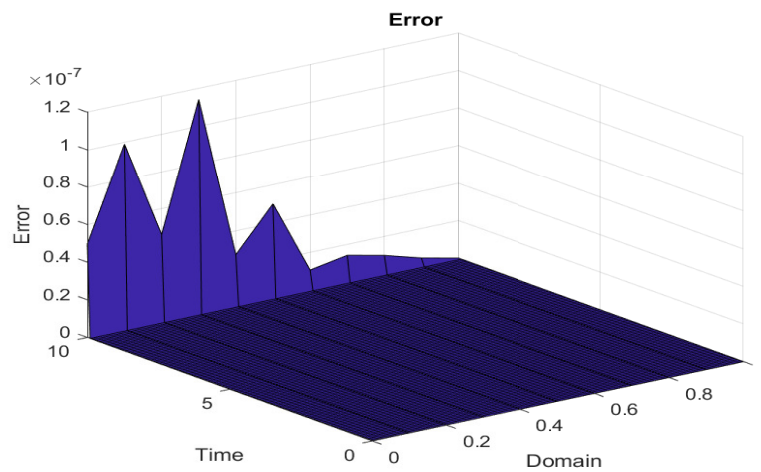


Figure 8. Error plot of Problem 3 at $\Delta t = 0.1, h = 0.1, t = 10$.

Table 6. L_R values for Example 3, when $N = 10, \Delta t = 0.1, t = 10$.

x/t	1	2	3	4	5	6	7
0	3.74×10^{-2}	7.26×10^{-3}	1.76×10^{-3}	3.99×10^{-4}	8.94×10^{-5}	2.00×10^{-5}	4.46×10^{-6}
0.2	1.53×10^{-2}	5.61×10^{-3}	1.34×10^{-3}	3.00×10^{-4}	6.53×10^{-5}	1.37×10^{-5}	2.63×10^{-6}
0.3	9.74×10^{-3}	4.89×10^{-3}	1.18×10^{-3}	2.72×10^{-4}	6.25×10^{-5}	1.47×10^{-5}	3.65×10^{-6}
0.4	6.18×10^{-3}	4.17×10^{-3}	1.00×10^{-3}	2.27×10^{-4}	5.02×10^{-5}	1.08×10^{-5}	2.21×10^{-6}
0.5	3.89×10^{-3}	3.44×10^{-3}	8.24×10^{-4}	1.87×10^{-4}	4.18×10^{-5}	9.40×10^{-6}	2.16×10^{-6}
0.6	2.42×10^{-3}	2.73×10^{-3}	6.55×10^{-4}	1.49×10^{-4}	3.34×10^{-5}	7.50×10^{-6}	1.68×10^{-6}
0.7	1.46×10^{-3}	2.03×10^{-3}	4.89×10^{-4}	1.11×10^{-4}	2.48×10^{-5}	5.53×10^{-6}	1.22×10^{-6}
0.8	8.16×10^{-4}	1.35×10^{-3}	3.24×10^{-4}	7.35×10^{-5}	1.64×10^{-5}	3.67×10^{-6}	8.20×10^{-7}
0.9	3.61×10^{-4}	6.73×10^{-4}	1.62×10^{-4}	3.66×10^{-5}	8.21×10^{-6}	1.84×10^{-6}	4.13×10^{-7}
1	0.00	0.00	0.00	0.000	0.00	0.00	0.00

x/t	8	9	10
0	9.94×10^{-7}	2.22×10^{-7}	4.95×10^{-8}
0.2	3.88×10^{-7}	7.20×10^{-9}	4.63×10^{-8}
0.3	9.96×10^{-7}	3.12×10^{-7}	1.14×10^{-7}
0.4	3.79×10^{-7}	2.32×10^{-8}	2.71×10^{-8}
0.5	5.29×10^{-7}	1.47×10^{-7}	4.99×10^{-8}
0.6	3.67×10^{-7}	7.40×10^{-8}	1.05×10^{-8}
0.7	2.69×10^{-7}	5.98×10^{-8}	1.41×10^{-8}
0.8	1.85×10^{-7}	4.23×10^{-8}	9.90×10^{-9}
0.9	9.20×10^{-8}	2.04×10^{-8}	4.30×10^{-9}
1	0.00	0.00	0.00

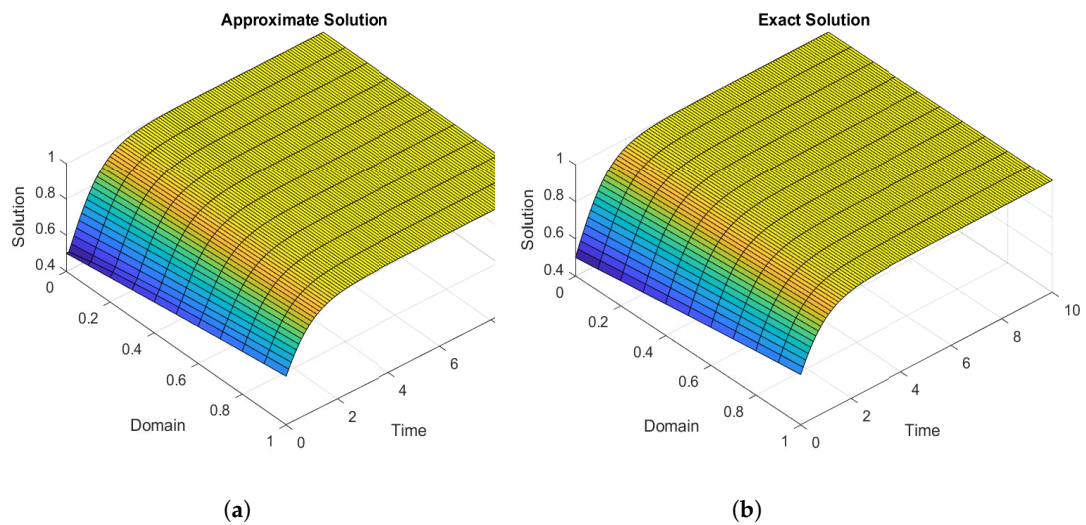


Figure 9. (a) Surface plot for the numerical solution of Problem 3, when $h = 0.1, t = 10$ (b) Surface plot for the exact solution when $t = 10, h = 0.1$.

5. Conclusions

In this work, a time-dependent equation involving the Allen–Cahn and PHI-Four models is studied and solved numerically, implementing the non-polynomial spline technique. The numerical results for three test problems are obtained to show efficiency of the suggested scheme. The approach involves the transformation of the PHI-Four equation into a coupled system of equations and finding a numerical solution for the aforementioned system. To achieve this, we employ the non-polynomial spline function for the spatial discretization and finite difference for time distribution. The results obtained clearly demonstrate that the current technique is viable and effective, providing accurate approximations to the solution. The obtained results with the suggested method show better accuracy than those obtained using the existing methods. The stability of the proposed scheme is discussed by way of von Neumann stability which indicates that the suggested method is unconditionally stable. A convergence test is carried out, and different orders of convergences for the scheme are obtained. The method is also tested for longer time $t \gg 0$

to show the effectiveness and viability of the suggested method at greater time values. We can conclude that the non-polynomial splines can be used as basis functions for different numerical techniques.

Author Contributions: Conceptualization, M.U.H. and S.H.; Methodology, M.U.H.; Software, M.U.H.; Validation, M.U.H. and S.H.; Formal analysis, S.H.; Investigation, M.U.H.; Resources, I.A.; Writing—original draft, M.U.H.; Visualization, I.A.; Supervision, S.H.; Funding acquisition, M.J.E. All authors have read and agreed to the published version of the manuscript.

Funding: This research received no external funding.

Data Availability Statement: The data used to support the findings of this study are available from the first author upon request.

Conflicts of Interest: The authors declare no conflicts of interest.

References

1. Triki, H.; Wazwaz, A.-M. Bright and dark soliton solutions for a $k(m, n)$ equation with t -dependent coefficients. *Phys. Lett. A* **2009**, *373*, 2162–2165. [CrossRef]
2. Zahra, W. Trigonometric b-spline collocation method for solving phi-four and allen–cahn equations. *Mediterr. J. Math.* **2017**, *14*, 1–19. [CrossRef]
3. Triki, H.; Wazwaz, A.-M. On soliton solutions for the fitzhugh–nagumo equation with time-dependent coefficients. *Appl. Math. Model.* **2013**, *37*, 3821–3828. [CrossRef]
4. Hariharan, G. An efficient legendre wavelet-based approximation method for a few newell–whitehead and allen–cahn equations. *J. Membr. Biol.* **2014**, *247*, 371–380. [CrossRef] [PubMed]
5. Hariharan, G.; Kannan, K. Haar wavelet method for solving cahn–allen equation. *Appl. Math. Sci.* **2009**, *3*, 2523–2533.
6. Beneš, M.; Chalupecký, V.; Mikula, K. Geometrical image segmentation by the allen–cahn equation. *Appl. Numer. Math.* **2004**, *51*, 187–205. [CrossRef]
7. Bhrawy, A.H.; Assas, L.M.; Alghamdi, M.A. An efficient spectral collocation algorithm for nonlinear phi-four equations. *Bound. Value Probl.* **2013**, *87*. [CrossRef]
8. Ehsani, F.; Hadi, A.; Hadi, N. Analytical solution of phi-four Equation. *Tech. J. Eng. Appl. Sci.* **2013**, *3*, 1378–1388.
9. Triki, H.; Wazwaz, A.-M. Envelope solitons for generalized forms of the phi-four Equation. *J. King Saud Univ.-Sci.* **2013**, *25*, 129–133. [CrossRef]
10. Alofi, A. Exact and explicit traveling wave solutions for the nonlinear partial differential equations. *World Appl. Sci. J.* **2013**, *21*, 62–67.
11. Soliman, A.; Abdo, H. New exact solutions of nonlinear variants of the rlw, the phi-four and boussinesq equations based on modified extended direct algebraic method. *arXiv* **2012**, arXiv:1207.5127.
12. Najafi, M. Using he’s variational method to seek the traveling wave solution of phi-four equation. *Int. J. Appl. Math. Res.* **2012**, *1*, 659–665. [CrossRef]
13. Ali, I.; Islam, S.; Siddique, I.; Min-Allah, N. Some efficient numerical solutions of allen–cahn equation with non-periodic boundary conditions. *Int. J. Nonlinear Sci.* **2011**, *11*, 380–384.
14. Schoenberg, I.J. Contributions to the problem of approximation of equidistant data by analytic functions. Part A. On the problem of smoothing or graduation. A first class of analytic approximation formulae. *Q. Appl. Math.* **1946**, *4*, 45–99. [CrossRef]
15. Ahlberg, J.H.; Nilson, E.N. Convergence properties of the spline fit. *J. Soc. Ind. Appl. Math.* **1963**, *11*, 95–104. [CrossRef]
16. Birkhoff, G.; Garabedian, H.L. Smooth surface interpolation. *J. Math. Phys.* **1960**, *39*, 258–268. [CrossRef]
17. Loscalzo, F.R.; Talbot, T.D. Spline function approximations for solutions of ordinary differential equations. *SIAM J. Numer. Anal.* **1967**, *4*, 433–445. [CrossRef]
18. Schultz, M.H.; Varga, R.S. L-splines. *Numer. Math.* **1967**, *10*, 345–369. [CrossRef]
19. Rubin, S.; Khosla, P. Higher-order numerical solutions using cubic splines. *AIAA J.* **1976**, *14*, 851–858. [CrossRef]
20. Schoenberg, I. Spline functions, convex curves and mechanical quadrature. *Bull. Am. Math. Soc.* **1958**, *64*, 352–357. [CrossRef]
21. Albasiny, E.; Hoskins, W. Cubic spline solutions to two-point boundary value Problems. *Comput. J.* **1969**, *12*, 151–153. [CrossRef]
22. Bickely, W. Piecewise cubic interpolation and two-point boundary value Problems. *Comput. J.* **1968**, *11*, 202–208.
23. Swaid, M. Lineer Denklem Sistemlerinin Sonlu Fark Metodu ve Non-polynomial Kübik Spline Metodu Yardımıyla Nümerik Çözümlerinin Elde Edilmesi. 2021. Available online: <https://hdl.handle.net/11413/6548> (accessed on 23 November 2021).
24. Jain, M.K.; Aziz, T. Spline function approximation for differential equations. *Comput. Methods Appl. Mech. Eng.* **1981**, *26*, 129–143. [CrossRef]
25. Jain, M.K.; Aziz, T. Cubic spline solution of two-point boundary value problems with significant first derivatives. *Comput. Methods Appl. Mech. Eng.* **1983**, *39*, 83–91. [CrossRef]
26. Usmani, R.A. The use of quartic splines in the numerical solution of a fourth-order boundary value problem. *J. Comput. Appl. Math.* **1992**, *44*, 187–200. [CrossRef]

27. Usmani, R.A.; Sakai, M. Quartic spline solutions for two-point boundary problems involving third order differential equations. *J. Math. Phys. Sci.* **1984**, *18*, 365–380.
28. Usmani, R.; Warsi, S. Quintic spline solutions of boundary value problems. *Comput. Math. Appl.* **1980**, *6*, 197–203. [[CrossRef](#)]
29. Noor, M.A.; Tirmizi, I.A.; Khan, M.A.; Khan, M.A. Quadratic non-polynomial spline approach to the solution of a system of second-order boundary-value problems. *Appl. Math. Comput.* **2006**, *179*, 153–160.
30. Tirmizi, I.A.; ul Islam, S. Nonpolynomial spline approach to the solution of a system of second-order boundary-value problems. *Appl. Math. Comput.* **2006**, *173*, 1208–1218.
31. ul Islam, S.; Tirmizi, I.A.; Haq, F. Quartic non-polynomial splines approach to the solution of a system of second-order boundary-value problems. *Int. J. High Perform. Comput. Appl.* **2007**, *21*, 42–49. [[CrossRef](#)]
32. Caglar, H.; Caglar, N. Fifth-degree b-spline solution for a fourth-order parabolic partial differential equations. *Appl. Math. Comput.* **2008**, *201*, 597–603. [[CrossRef](#)]
33. Rashidinia, J.; Mahmoodi, Z. Non-polynomial spline solution of a singularly-perturbed boundary-value problems. *Int. J. Contemp. Math. Sci.* **2007**, *2*, 1581–1586. [[CrossRef](#)]
34. Tirmizi, I.A.; ul Islam, S.; Hap, F. Non-polynomial spline solution of singularly perturbed boundary-value problems. *Appl. Math. Comput.* **2008**, *196*, 6–16. [[CrossRef](#)]
35. Khan, M.A.; ul Islam, S. A numerical method based on polynomial sextic spline functions for the solution of special fifth-order boundary-value problems. *Appl. Math. Comput.* **2006**, *181*, 356–361.
36. Siddiqi, S.S.; Akram, G. Solution of fifth order boundary value problems using nonpolynomial spline technique. *Appl. Math. Comput.* **2006**, *175*, 1574–1581. [[CrossRef](#)]
37. Siddiqi, S.S.; Akram, G.; Malik, S.A. Nonpolynomial sextic spline method for the solution along with convergence of linear special case fifth-order two-point boundary value problems. *Appl. Math. Comput.* **2007**, *190*, 532–541. [[CrossRef](#)]
38. Akram, G.; Siddiqi, S.S. Solution of sixth order boundary value problems using non-polynomial spline technique. *Appl. Math. Comput.* **2006**, *181*, 708–720. [[CrossRef](#)]
39. Ramadan, M.A.; El-Danaf, T.S.; Alaal, F.E.A. Application of the non-polynomial spline approach to the solution of the burgers' equation. *Open Appl. Math. J.* **2007**, *1*, 15–20. [[CrossRef](#)]
40. Rashidinia, J.; Mohammadi, R. Non-polynomial cubic spline methods for the solution of parabolic equations. *Int. J. Comput. Math.* **2008**, *85*, 843–850. [[CrossRef](#)]
41. Viswanadham, K.K.; Ballem, S. Numerical solution of eighth order boundary value problems by galerkin method with quintic b-splines. *Int. J. Comput. Appl.* **2013**, *975*, 8887.
42. Alam, M.; Haq, S.; Ali, I.; Ebadi, M.J.; Salahshour, S. Radial basis functions approximation method for time-fractional fitzhugh–nagumo equation. *Fractal Fract.* **2023**, *7*, 882. [[CrossRef](#)]
43. Radmanesh, M.; Ebadi, M.J. A local meshless radial basis functions based method for solving fractional integral equations. *Comput. Algorithms Numer. Dimens.* **2023**, *2*, 35–46.
44. Avazzadeh, Z.; Hassani, H.; Agarwal, P.; Mehrabi, S.; Ebadi, M.J.; Asl, M.K.H. Optimal study on fractional fascioliasis disease model based on generalized fibonacci polynomials. *Math. Methods Appl. Sci.* **2023**, *46*, 9332–9350. [[CrossRef](#)]
45. Schweikert, D.G. An interpolation curve using a spline in tension. *J. Math. Phys.* **1966**, *45*, 312–317. [[CrossRef](#)]
46. Pruess, S. Properties of splines in tension. *J. Approx. Theory* **1976**, *17*, 86–96. [[CrossRef](#)]
47. Madzvamuse, A.; Maini, P.K. Velocity-induced numerical solutions of reaction-diffusion systems on continuously growing domains. *J. Comput. Phys.* **2007**, *225*, 100–119. [[CrossRef](#)]

Disclaimer/Publisher's Note: The statements, opinions and data contained in all publications are solely those of the individual author(s) and contributor(s) and not of MDPI and/or the editor(s). MDPI and/or the editor(s) disclaim responsibility for any injury to people or property resulting from any ideas, methods, instructions or products referred to in the content.